Electronic Supplementary Material (ESI) for Physical Chemistry Chemical Physics.

Confinement Dependence of Protein-Associated Solvent Dynamics around Different Classes of Proteins, from the EPR Spin Probe Perspective

Wei Li, Katie Lynn Whitcomb and Kurt Warncke

Department of Physics, Emory University, Atlanta, Georgia 30322

Supplementary Information

Table of Contents

Table S3-S7. Mean $\log \tau_c$ and W values at different T values, under weak confinement, in the presence of added DMSO cryosolvent for proteins: SA, Mb, Cas, PRM, and Aβ16.

Table S8-S12. Mean $\log \tau_c$ and W values at different T values, under strong confinement, in the absence of cryosolvent for proteins: SA, Mb, Cas, PRM, and Aβ16.

Table S13. Arrhenius parameters for TEMPOL rotational correlation times for Region III and boundary T values under weak confinement, in the presence of added DMSO.

Table S14. Arrhenius parameters for TEMPOL rotational correlation times for Region III and boundary T values under strong confinement, in the absence of added cryosolvent.

Table S15. Calculated protein rotational correlation times for solution at room temperature and in the mesodomain at 240 K.

SI References

SI Figures

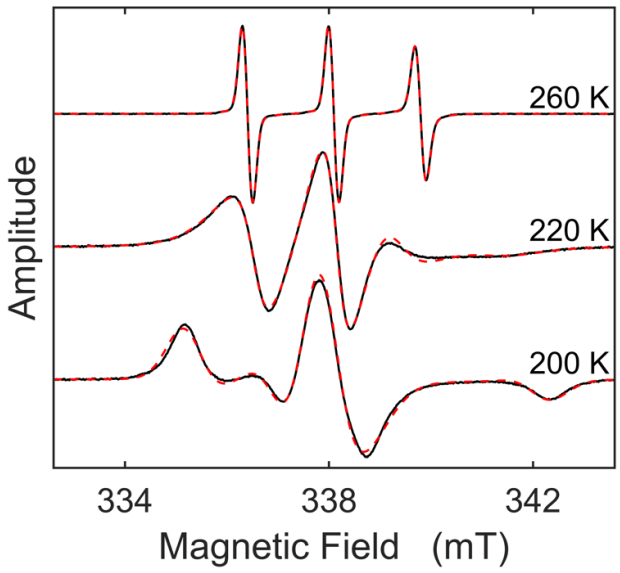

Figure S1. Single component TEMPOL EPR spectra in frozen aqueous solution with added 2% v/v DMSO, in the absence of protein. Experimental spectra (black) show the three general line shape regimes of rigid limit (200 K), intermediate rotational mobility (220 K) and rapid tumbling (260 K). EPR spectra, simulated under the assumption of random rotational motion about the three Cartesion axes, by using the rotational correlation time predicted from the Debye-Stokes-Einstein theory for viscosity-dependent rotational diffusion, are shown overlaid (red). The predicted correlation times are presented in Table S1.

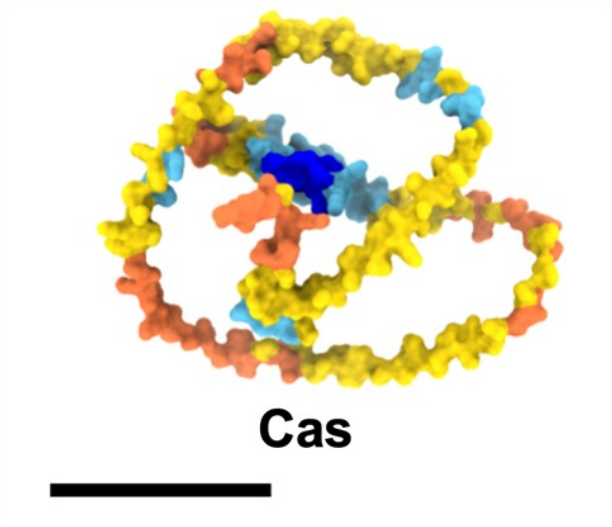

Figure S2. Depiction of the amino acid sequence of β-casein (Cas), showing degree of structure prediction certainty (color code: very low, orange; low, yellow; high, blue; very high, dark blue) by AlphaFold[1] (uniprot database,[2] P02666; bovine, *Bos taurus*). Scale bar is 50 Å in length.

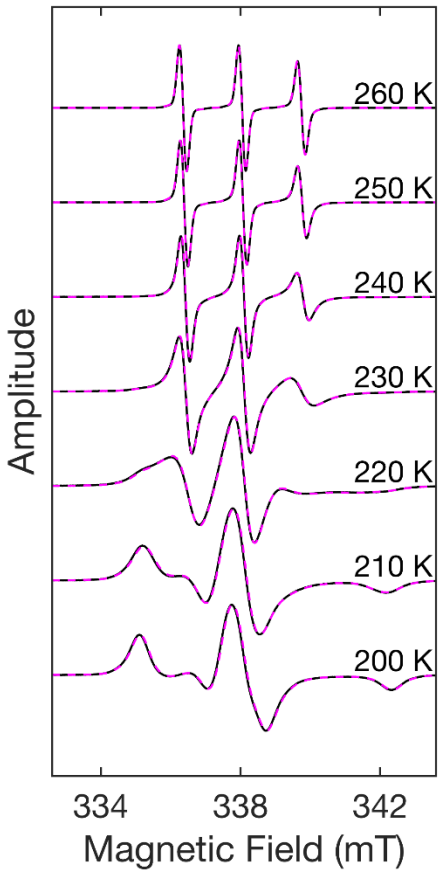

Figure S3. Temperature dependence of the TEMPOL EPR spectrum in the presence of streptavidin and streptavidin plus 4 equivalents of biotin per binding site under the weak confinement condition (added 2% DMSO). Spectrum of streptavidin plus biotin (magenta, dashed) is overlaid on streptavidin-only spectrum (black). Conditions are the same as for Figure 3, and as described in Materials and Methods.

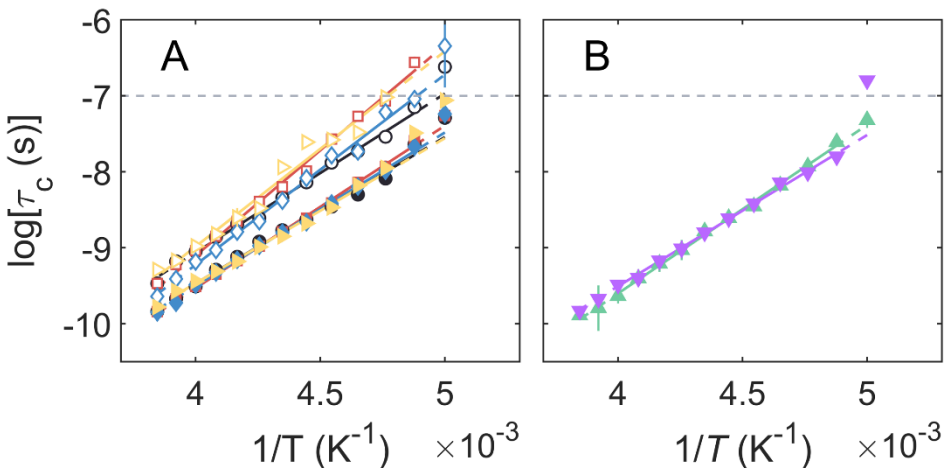

Figure S4. Arrhenius plots of the TEMPOL rotational correlation times for Region III, under the weak confinement condition, in the presence of added DMSO. The plots show data for the slow component ($\log \tau_{c,s}$, open symbol) and fast component ($\log \tau_{c,f}$, filled symbol), and linear fits (solid line) for Region III and boundary T values (T range shown in Figure 4; 205-250 K for all, except Cas, 210-255 K), with extrapolations to neighbor regions (dashed line). (A) EAL (black, circles),[3] SA (red, squares), Mb (blue, diamonds), and Cas (gold, triangles). (B) Pro (green, triangles, base down) and Aβ16 (violet, triangles, base up). The horizontal dashed line represents the upper limit of $\log \tau_c = -7.0$ for detection of TEMPOL motion. Errror bars represent standard deviations from three separate determinations.

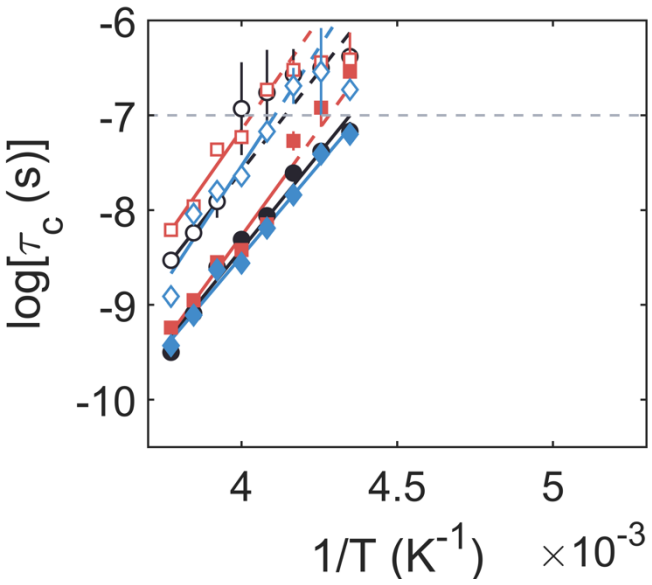

Figure S5. Arrhenius plots of the TEMPOL rotational correlation times for Region III, under the strong confinement condition, in the absence of DMSO. The plots show data for the slow component ($\log \tau_{c,s}$, open symbol) and fast component ($\log \tau_{c,f}$, filled symbol), and linear fits (solid line) for Region III and boundary T value range, shown in Figure 5; $\log \tau_c < -7.0$, with extrapolations to neighbor regions (dashed line). EAL (black, circles),[3] SA (red, squares), and Mb (blue, diamonds). The horizontal dashed line represents the upper limit of $\log \tau_c = -7.0$ for detection of TEMPOL motion. Errror bars represent standard deviations from three separate determinations.

SI Tables

Table S1. Experimental and calculated rotational correlation times for TEMPOL in the mesodomain in frozen solution with added 2% DMSO in the absence of protein, and viscosity, η, of the maximum freeze-concentrated aqueous-DMSO solution, at temperatures representative of canonical regimes of spin label motion: rigid limit (200 K), intermediate rotational mobility (220 K) and rapid tumbling (260 K).

T (K)	η (P)	$\log[\tau_{c,\,SE}\ (s)]$	$\log[\tau_{c,\,SIM}\ (s)]$
260	0.17	-9.86	-9.86
220	2.84	-8.57	-8.48
200	31.80	-7.48	-7.34

[a] The correlation times, $\tau_{c,SIM}$, are obtained from simulation of the EPR spectra presented in Figure S1.

[b] The correlation times, $\tau_{c,SE}$, are calculated by using the Debye-Stokes-Einstein theory,[1] and the viscosity, η, of the maximum freeze-concentrated aqueous-DMSO phase, at each temperature.[2]

Table S2. EPR sample protein parameters and mesodomain parameters.[a]

Protein / Parameter	EAL	SA	Mb	Cas	PRM	Ab16
PDB ID[b]	5ysn	3ry1	1u7s	-	-	1ze7
AlphaFold ID[b]	-	-	-	P02666	P69014	-
M_r (kDa)[c]	488	52.8	16.7	24.0	4.36	1.96
[protein] (mM)	20.0	131	80.8	21.0[d]	386	787
n_{prot}	3.61×10^{15}	2.37×10^{16}	1.46×10^{16}	3.79×10^{15}	6.97×10^{16}	1.42×10^{17}
ASA (Å^2)[e]	1.36×10^{5}	2.08×10^{4}	8.40×10^{3}	-[f]	-[g]	1.71×10^{3}
ASA_{tot} (Å^2)	4.91×10^{20}	4.92×10^{20}	1.23×10^{20}	-[f]	-[g]	2.43×10^{20}
DMSO present						
V_{meso} (mL)[h]	9.23	9.23	2.31	0.33[d]	9.23	9.23
$<t_{meso}>$ (Å)	18.8	18.8	18.8	-[i]	-[j]	38.0[k]

Footnotes

[a] The protein concentration ([protein]) and number of proteins (n_{prot}), accessible surface area per protein (ASA) and total protein accessible surface area in the sample (ASA_{tot}) are identical for EPR samples in the presence (weak confinement) and absence (strong confinement) of added dimethylsulfoxide (DMSO) cryosolvent. The volume of aqueous-DMSO phase (V_{meso}) and mean mesodomain thickness ($<t_{meso}>$) refer to samples prepared in the presence of DMSO.

[b] Identification codes for the protein data bank (PDB)[4] structure and AlphaFold[1, 5] predicted structure files

[c] M_r, molecular mass

[d] The relatively low concentration of Cas (and attendant low volume of DMSO) adhere to the low solubility limit of Cas in aqueous solution.[6]

[e] ASA is determined by using Virtual Molecular Dynamics, VMD.[7]

f The value of ASA and ASA_{tot} for Cas are less certain than for the folded proteins of known structure, because of its intrinsically disordered protein (IDP) nature. Lower limits of ASA=4.62×10^3 Å^2 and ASA_{tot}=1.75×10^{19} Å^2 are obtained by using the surface area of the volume of the equivalent sphere of protein mass (assumed protein density 1.35 mg/ml[8, 9]). Upper limits of ASA=2.82×10^4 Å^2 and ASA_{tot}=1.07×10^{20} Å^2 are obtained from the AlphaFold prediction (P02666) by using VMD.

g The value of ASA and ASA_{tot} for PRM are less certain than for the folded proteins of known structure, because of its intrinsically disordered protein (IDP) nature. Lower limits of ASA=1.52×10^3 Å^2 and ASA_{tot}=1.06×10^{20} Å^2 are obtained by using the surface area of the volume of the equivalent sphere of protein mass (assumed protein density 1.35 mg/ml [8 9]). Upper limits of ASA=6.14×10^3 Å^2 and ASA_{tot}=4.28×10^{20} Å^2 are obtained from the AlphaFold prediction (P69014) by using VMD.

h The volume of the aqueous-DMSO mesodomain, V_{meso}, is estimated from V_{DMSO}/g_{meso}, where V_{DMSO} is the volume of DMSO added to the sample, and g_{meso} is the fractional maximum freeze concentration of DMSO, 0.65.[3, 10]

i The $<t_{meso}>$ values corresponding to lower and upper limits of the ASA (see footnote **e**) are 18.8 and 3.1 Å, respectively. A $<t_{meso}>$ within this range is in accord with the observed +5 K shift in Region II/III (ODT) and III/IV boundaries for Cas, relative to the globular proteins.

j The $<t_{meso}>$ values corresponding to lower and upper limits of the ASA (see footnote **f**) are 87 and 21.6 Å, respectively.

k The value of 38 Å represents an upper limit, relative to more extended conformers in the repertoire of Aβ16 NMR structures.[11]

Table S3. Mean logτ_c and W values at different T values, under weak confinement, in the presence of added DMSO cryosolvent: SA

T (K)	log $\tau_{c,s}$ (s)	W_s	log $\tau_{c,f}$ (s)	W_f
200	-5.76 ± 0.05	0.13 ± 0.10	-7.26 ± 0.09	0.87 ± 0.10
205	-6.56 ± 0.30	0.18 ± 0.10	-7.59 ± 0.08	0.81 ± 0.10
210	-7.07 ± 0.05	0.27 ± 0.04	-7.93 ± 0.02	0.60 ± 0.07
215	-7.27 ± 0.06	0.20 ± 0.01	-8.14 ± 0.05	0.70 ± 0.08
220	-7.57 ± 0.10	0.25 ± 0.04	-8.41 ± 0.01	0.75 ± 0.04
225	-7.99 ± 0.07	0.28 ± 0.03	-8.61 ± 0.01	0.72 ± 0.03
230	-8.20 ± 0.05	0.26 ± 0.02	-8.79 ± 0.01	0.74 ± 0.02
235	-8.39 ± 0.06	0.22 ± 0.02	-8.98 ± 0.01	0.78 ± 0.02
240	-8.65 ± 0.21	0.25 ± 0.05	-9.17 ± 0.01	0.75 ± 0.05
245	-8.85 ± 0.12	0.25 ± 0.02	-9.35 ± 0.01	0.75 ± 0.02
250	-9.04 ± 0.07	0.23 ± 0.01	-9.51 ± 0.01	0.77 ± 0.01
255	-9.22 ± 0.08	0.21 ± 0.01	-9.67 ± 0.01	0.79 ± 0.01
260	-9.47 ± 0.05	0.19 ± 0.01	-9.84 ± 0.01	0.81 ± 0.01

Table S4. Mean logτ_c and W values at different T values, under weak confinement, in the presence of added DMSO cryosolvent: Mb

T (K)	log $\tau_{c,s}$ (s)	W_s	log $\tau_{c,f}$ (s)	W_f
200	-6.35 ± 0.55	0.08 ± 0.02	-7.24 ± 0.05	0.92 ± 0.02
205	-6.04 ± 0.05	0.29 ± 0.00	-7.67 ± 0.01	0.71 ± 0.00
210	-7.22 ± 0.05	0.28 ± 0.01	-7.98 ± 0.00	0.72 ± 0.01
215	-7.73 ± 0.02	0.29 ± 0.00	-8.19 ± 0.01	0.71 ± 0.00
220	-7.79 ± 0.03	0.25 ± 0.02	-8.42 ± 0.01	0.75 ± 0.02
225	-8.08 ± 0.08	0.31 ± 0.02	-8.67 ± 0.03	0.69 ± 0.02
230	-8.38 ± 0.02	0.29 ± 0.02	-8.80 ± 0.01	0.71 ± 0.02
235	-8.65 ± 0.08	0.30 ± 0.04	-8.97 ± 0.00	0.70 ± 0.04
240	-8.79 ± 0.11	0.29 ± 0.03	-9.16 ± 0.00	0.71 ± 0.03
245	-9.03 ± 0.04	0.29 ± 0.01	-9.33 ± 0.00	0.71 ± 0.01
250	-9.18 ± 0.07	0.28 ± 0.01	-9.49 ± 0.01	0.72 ± 0.01
255	-9.41 ± 0.05	0.29 ± 0.03	-9.73 ± 0.05	0.71 ± 0.03
260	-9.64 ± 0.00	0.26 ± 0.01	-9.85 ± 0.00	0.74 ± 0.01

Table S5. Mean logτ_c and W values at different T values, under weak confinement, in the presence of added DMSO cryosolvent: Cas

T (K)	log $\tau_{c,s}$ (s)	W_s	log $\tau_{c,f}$ (s)	W_f
200	-4.83 ± 0.32	0.02 ± 0.00	-7.06 ± 0.04	0.98 ± 0.00
205	-4.43 ± 0.27	0.16 ± 0.04	-7.49 ± 0.06	0.84 ± 0.04
210	-7.02 ± 0.06	0.38 ± 0.04	-7.95 ± 0.01	0.62 ± 0.04
215	-7.48 ± 0.06	0.44 ± 0.01	-8.18 ± 0.04	0.56 ± 0.01
220	-7.58 ± 0.02	0.40 ± 0.01	-8.47 ± 0.03	0.60 ± 0.01
225	-7.61 ± 0.02	0.42 ± 0.02	-8.68 ± 0.02	0.58 ± 0.02
230	-7.94 ± 0.06	0.44 ± 0.01	-8.85 ± 0.06	0.56 ± 0.01
235	-8.48 ± 0.01	0.45 ± 0.02	-8.99 ± 0.02	0.55 ± 0.02
240	-8.60 ± 0.12	0.44 ± 0.03	-9.18 ± 0.02	0.56 ± 0.03
245	-8.82 ± 0.06	0.42 ± 0.04	-9.31 ± 0.01	0.58 ± 0.04
250	-8.98 ± 0.07	0.41 ± 0.05	-9.44 ± 0.00	0.59 ± 0.05
255	-9.17 ± 0.05	0.40 ± 0.06	-9.57 ± 0.00	0.60 ± 0.00
260	-9.29 ± 0.05	0.36 ± 0.03	-9.78 ± 0.01	0.64 ± 0.00
265	-9.65 ± 0.04	0.36 ± 0.02	-9.65 ± 0.00	0.64 ± 0.00

Table S6. Mean logτ_c values at different T values, under weak confinement, in the presence of added DMSO cryosolvent: PRM

T (K)	log τ_c (s)
200	-7.32 ± 0.10
205	-7.61 ± 0.05
210	-7.93 ± 0.00
215	-8.18 ± 0.00
220	-8.38 ± 0.01
225	-8.61 ± 0.01
230	-8.78 ± 0.00
235	-9.03 ± 0.13
240	-9.21 ± 0.11
245	-9.40 ± 0.05
250	-9.63 ± 0.10
255	-9.79 ± 0.30
260	-9.89 ± 0.02

Table S7. Mean logτ_c values at different T values, under weak confinement, in the presence of added DMSO cryosolvent: Aβ16

T (K)	log τ_c (s)
200	-6.80 ± 0.10
205	-7.80 ± 0.05
210	-8.01 ± 0.00
215	-8.14 ± 0.00
220	-8.42 ± 0.01
225	-8.61 ± 0.01
230	-8.80 ± 0.00
235	-9.01 ± 0.13
240	-9.17 ± 0.11
245	-9.40 ± 0.05
250	-9.49 ± 0.10
255	-9.67 ± 0.30
260	-9.83 ± 0.02

Table S8. Mean logτ_c and W values at different T values, under strong confinement, in the absence of added DMSO cryosolvent: SA

T (K)	log $\tau_{c,s}$ (s)	W_s	log $\tau_{c,f}$ (s)	W_f
230	-6.41 ± 0.08	0.10 ± 0.04	-6.72 ± 0.28	0.90 ± 0.04
235	-6.44 ± 0.11	0.11 ± 0.03	-6.86 ± 0.20	0.89 ± 0.03
240	-6.52 ± 0.10	0.15 ± 0.02	-7.39 ± 0.10	0.85 ± 0.02
245	-6.73 ± 0.04	0.70 ± 0.00	-8.18 ± 0.03	0.30 ± 0.00
250	-7.23 ± 0.04	0.67 ± 0.01	-8.43 ± 0.06	0.33 ± 0.01
255	-7.36 ± 0.15	0.70 ± 0.06	-8.55 ± 0.06	0.30 ± 0.06
260	-7.96 ± 0.01	0.76 ± 0.01	-8.96 ± 0.01	0.24 ± 0.01
265	-8.21 ± 0.05	0.72 ± 0.06	-9.29 ± 0.07	0.28 ± 0.06

Table S9. Mean logτ_c and W values at different T values, under strong confinement, in the absence of added DMSO cryosolvent: Mb

T (K)	log $\tau_{c,s}$ (s)	W_s	log $\tau_{c,f}$ (s)	W_f
230	-6.73 ± 0.07	0.14 ± 0.01	-7.20 ± 0.07	0.86 ± 0.01
235	-6.54 ± 0.46	0.26 ± 0.01	-7.41 ± 0.01	0.74 ± 0.01
240	-6.69 ± 0.19	0.35 ± 0.05	-7.84 ± 0.06	0.65 ± 0.05
245	-7.17 ± 0.01	0.51 ± 0.02	-7.19 ± 0.01	0.49 ± 0.02
250	-7.64 ± 0.02	0.69 ± 0.01	-8.56 ± 0.03	0.31 ± 0.01
255	-7.80 ± 0.01	0.69 ± 0.01	-8.63 ± 0.08	0.31 ± 0.01
260	-8.04 ± 0.01	0.68 ± 0.00	-9.11 ± 0.05	0.32 ± 0.00
265	-8.91 ± 0.01	0.56 ± 0.01	-9.43 ± 0.00	0.44 ± 0.01

Table S10. Mean logτ_c and W values at different T values, under strong confinement, in the absence of added DMSO cryosolvent: Cas

T (K)	log $\tau_{c,s}$ (s)	W_s	log $\tau_{c,f}$ (s)	W_f
230	-5.42 ± 0.17	0.03 ± 0.00	-7.01 ± 0.03	0.97 ± 0.00
235	-5.80 ± 0.16	0.05 ± 0.01	-7.33 ± 0.09	0.95 ± 0.01
240	-6.44 ± 0.09	0.10 ± 0.02	-7.62 ± 0.09	0.90 ± 0.02
245	-7.00 ± 0.07	0.24 ± 0.09	-7.94 ± 0.13	0.76 ± 0.09
250	-7.37 ± 0.03	0.39 ± 0.03	-8.30 ± 0.06	0.61 ± 0.03
255	-7.91 ± 0.07	0.69 ± 0.04	-8.67 ± 0.08	0.31 ± 0.04
260	-8.14 ± 0.04	0.62 ± 0.09	-8.93 ± 0.03	0.38 ± 0.09
265	-8.57 ± 0.00	0.54 ± 0.00	-9.23 ± 0.00	0.46 ± 0.00

Table S11. Mean logτ_c and W values at different T values, under strong confinement, in the absence of added DMSO cryosolvent: PRM

T (K)	log $\tau_{c,s}$ (s)	W_s	log $\tau_{c,f}$ (s)	W_f
250	-6.70 ± 0.18	0.98 ± 0.01	-8.79 ± 0.04	0.02 ± 0.01
255	-7.13 ± 0.06	0.95 ± 0.00	-9.29 ± 0.04	0.05 ± 0.00
260	-7.80 ± 0.09	0.80 ± 0.02	-9.37 ± 0.06	0.20 ± 0.02
265	-8.69 ± 0.13	0.53 ± 0.04	-9.60 ± 0.04	0.47 ± 0.04

Table S12. Mean logτ_c and W values at different T values, under strong confinement, in the absence of added DMSO cryosolvent: Aβ16

T (K)	log $\tau_{c,s}$ (s)	W_s	log $\tau_{c,f}$ (s)	W_f
230	-5.82 ± 0.27	0.06 ± 0.00	-6.99 ± 0.06	0.94 ± 0.00
235	-5.83 ± 0.29	0.25 ± 0.18	-7.39 ± 0.14	0.75 ± 0.18
240	-6.79 ± 0.07	0.73 ± 0.01	-8.10 ± 0.05	0.27 ± 0.01
245	-7.23 ± 0.04	0.72 ± 0.01	-8.41 ± 0.05	0.28 ± 0.01
250	-7.63 ± 0.05	0.83 ± 0.01	-8.93 ± 0.03	0.17 ± 0.01
255	-7.72 ± 0.07	0.67 ± 0.02	-9.03 ± 0.05	0.33 ± 0.02
260	-7.78 ± 0.04	0.44 ± 0.03	-9.30 ± 0.01	0.56 ± 0.03
265	-9.25 ± 0.01	0.32 ± 0.01	-9.70 ± 0.01	0.48 ± 0.01

Table S13. Arrhenius parameters for TEMPOL rotational correlation times for Region III and boundary *T* values under weak confinement, in the presence of added DMSO.[a]

protein	-log $\tau_{c,s0}$ (s)	$E_{a,s}$ (kcal/mol)	-log $\tau_{c,f0}$ (s)	$E_{a,f}$ (kcal/mol)
EAL [b]	17.4 ± 0.60	9.57 ± 0.62	17.2 ± 0.85	8.80 ± 0.88
SA	20.2 ± 0.84	12.7 ± 0.86	18.1 ± 0.37	9.78 ± 0.38
Mb	19.2 ± 0.86	11.4 ± 0.88	17.6 ± 0.37	9.24 ± 0.38
Cas	19.3 ± 1.52	11.6 ± 0.60	17.1 ± 0.55	8.74 ± 0.59
PRM[c]	-	-	18.5 ± 0.42	10.1 ± 0.44
Aβ16[c]	-	-	17.5 ± 0.42	9.10 ± 0.43

[a] Standard deviations are obtained from the fit to the data points, that correspond to the average of three determinations at each *T* value, as plotted in Figure S4.

[b] Temperature dependence of parameters determined previously.[1]

[c] A slow, PAD component is not detected for PRM and Aβ16 under weak confinement

Table S14. Arrhenius parameters for TEMPOL rotational correlation times for Region III and boundary *T* values under strong confinement, in the absence of added cryosolvent.[a]

protein	-log $\tau_{c,s0}$ (s)	$E_{a,s}$ (kcal/mol)	-log $\tau_{c,f0}$ (s)	$E_{a,f}$ (kcal/mol)
EAL[b]	24.3 ± 5.35	19.2 ± 6.36	24.6 ± 2.45	18.6 ± 2.77
SA	25.9 ± 13.9	21.4 ± 16.3	26.4 ± 6.57	20.7 ± 7.57
Mb	27.6 ± 11.8	22.9 ± 13.7	24.1 ± 1.67	17.8 ± 1.88

[a] Standard deviations are obtained from the fit to the data points in Region III, that correspond to the average of three determinations at each *T* value, as plotted in Figure S5.

[b] Temperature dependence of parameters determined previously.[12]

Table S15. Calculated protein rotational correlation times for solution at room temperature and under weak confinement conditions in the aqueous-DMSO (2% v/v) mesodomain at 240 K.[a, b]

	log τ_c (s), 293 K	**log τ_c (s), 240 K**
EAL	-6.83	-5.04
Aβ16	-9.09	-7.31
TEMPOL	-10.15	-8.36

[a] The correlation times, τ_c, are calculated by using the Debye-Stokes-Einstein theory.[13] Viscosity at 293 K corresponds to pure water. Viscosity at 240 K was calculated[3] by using *T*-dependence of the viscosity of aqueous-DMSO solutions.[14]

[b] The molecular model is the sphere of equivalent volume, obtained from the molecular mass and density (1.35 mg/ml for the proteins[8, 9]).

SI References

1. J. Jumper, R. Evans, A. Pritzel, T. Green, M. Figurnov, O. Ronneberger, K. Tunyasuvunakool, R. Bates, A. Zidek, A. Potapenko, A. Bridgland, C. Meyer, S. A. A. Kohl, A. J. Ballard, A. Cowie, B. Romera–Paredes, S. Nikolov, R. Jain, J. Adler, T. Back, S. Petersen, D. Reiman, E. Clancy, M. Zielinski, M. Steinegger, M. Pacholska, T. Berghammer, S. Bodenstein, D. Silver, O. Vinyals, A. W. Senior, K. Kavukcuoglu, P. Kohli and D. Hassibis, *Nature*, 2021, **596**, 583–589.

2. CSN2 – Beta–casein precursor – Bos taurus (Bovine) – CSN2 gene & protein, www.uniprot.org/uniprot/P0266).

3. B. Nforneh and K. Warncke, *J. Phys. Chem. B*, 2019, **123**, 5395–5404.

4. H. M. Berman, J. Westbrook, Z. Feng, G. Gilliland, T. N. Bhat, H. Weissig, I. N. Shindyalov and P. E. Bourne, *Nucleic Acids Res.*, 2000, **28**, 235–242.

5. M. Varadi, S. Anyango, M. Deshpande, S. Nair, C. Natassia, G. Yordanova, D. Yuan, O. Stroe, G. Wood, A. Laydon, A. Zidek, T. Green, K. Tunyasuvunakool, S. Petersen, J. Jumper, E. Clancy, R. Green, A. Vora, M. Lutfi, M. Figurnov, A. Cowie, N. Hobbs, P. Kohli, G. Kleywegt, E. Birney, D. Hassibis and S. Velankar, *Nucleic Acids Res.*, 2022, **50**, D439–D444.

6. S. Ossowski, A. Jackson, M. Obiols–Rabasa, C. Holt, S. Lenton, L. Porcar, M. Paulsson and T. Nylander, *Langmuir*, 2012, **28**, 13577–13589.

7. W. Humphrey, A. Dahlke and K. Schulten, *J. Molec. Graphics*, 1996, **14**, 33–38.

8. M. L. Quillin and B. W. Matthews, *Acta Crystallogr. D Biol. Crystallog.*, 2000, **56**, 791–794.

9. H. Fischer, I. Polikarpov and A. F. Craievich, *Prot. Sci.*, 2004, **13**, 2825–2828.

10. W. Li, B. Nforneh, K. L. Whitcomb and K. Warncke, *Methods Enzymol.*, 2022, **666**, 25–57.

11. Z. Severine, S. A. Kozin, A. K. Mazur, A. Blond, M. Cheminant, I. Segalas–Milazzo, P. Debey and S. Rebuffat, *J. Biol. Chem.*, 2006, **281**, 2151–2161.

12. B. Nforneh and K. Warncke, *J. Phys. Chem. B*, 2017, **121**, 11109–11118.

13. H. Sato, S. E. Bottle, J. P. Blinco, A. S. Micallef, G. R. Eaton and S. S. Eaton, *J. Magn. Reson.*, 2008, **191**, 66–77.

14. S. A. Schichman and R. L. Amey, *J. Phys. Chem.*, 1971, **75**, 98–102.